HAL
open science

Thermodynamics of radicicol binding to human Hsp90 alpha and beta isoforms

Asta Zubrienė, Malgorzata Gutkowska, Jurgita Matulienė, Romanas Chaleckis, Vilma Michailovienė, Aliona Voroncova, Česlovas Venclovas, Alicja Zylicz, Maciej Zylicz, Daumantas Matulis

To cite this version:

Asta Zubrienė, Malgorzata Gutkowska, Jurgita Matulienė, Romanas Chaleckis, Vilma Michailovienė, et al.. Thermodynamics of radicicol binding to human Hsp90 alpha and beta isoforms. Biophysical Chemistry, 2010, 152 (1-3), pp.153. 10.1016/j.bpc.2010.09.003 . hal-00694295

HAL Id: hal-00694295

https://hal.science/hal-00694295v1

Submitted on 4 May 2012

HAL is a multi-disciplinary open access archive for the deposit and dissemination of scientific research documents, whether they are published or not. The documents may come from teaching and research institutions in France or abroad, or from public or private research centers.

L'archive ouverte pluridisciplinaire **HAL**, est destinée au dépôt et à la diffusion de documents scientifiques de niveau recherche, publiés ou non, émanant des établissements d'enseignement et de recherche français ou étrangers, des laboratoires publics ou privés.

Accepted Manuscript

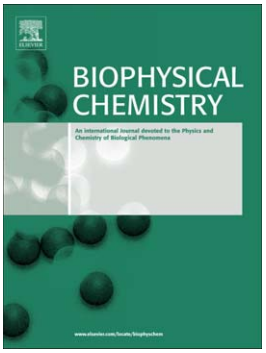

Thermodynamics of radicicol binding to human Hsp90 alpha and beta isoforms

Asta Zubriene, Malgorzata Gutkowska, Jurgita Matuliene, Romanas Chaleckis, Vilma Michailoviene, Aliona Voroncova, Ceslovas Venclovas, Alicja Zylicz, Maciej Zylicz, Daumantas Matulis

PII: S0301-4622(10)00227-9
DOI: doi: 10.1016/j.bpc.2010.09.003
Reference: BIOCHE 5429

To appear in: *Biophysical Chemistry*

Received date: 7 July 2010
Revised date: 14 September 2010
Accepted date: 15 September 2010

Please cite this article as: Asta Zubriene, Malgorzata Gutkowska, Jurgita Matuliene, Romanas Chaleckis, Vilma Michailoviene, Aliona Voroncova, Ceslovas Venclovas, Alicja Zylicz, Maciej Zylicz, Daumantas Matulis, Thermodynamics of radicicol binding to human Hsp90 alpha and beta isoforms, *Biophysical Chemistry* (2010), doi: 10.1016/j.bpc.2010.09.003

This is a PDF file of an unedited manuscript that has been accepted for publication. As a service to our customers we are providing this early version of the manuscript. The manuscript will undergo copyediting, typesetting, and review of the resulting proof before it is published in its final form. Please note that during the production process errors may be discovered which could affect the content, and all legal disclaimers that apply to the journal pertain.

ACCEPTED MANUSCRIPT

Thermodynamics of radicicol binding to human Hsp90 alpha and beta isoforms

Asta Zubrienė[1], Malgorzata Gutkowska[2,3], Jurgita Matulienė[1], Romanas Chaleckis[1], Vilma Michailovienė[1], Aliona Voroncova[1], Česlovas Venclovas[4], Alicja Zylicz[2], Maciej Zylicz[2], and Daumantas Matulis[1]

[1] Laboratory of Biothermodynamics and Drug Design, Institute of Biotechnology, LT-02241 Vilnius, Lithuania

[2] International Institute of Molecular and Cell Biology in Warsaw, 02-109 Warsaw, Poland

[3] The Nencki Institute of Experimental Biology, 02-093 Warsaw, Poland

[4] Laboratory of Bioinformatics, Institute of Biotechnology, LT-02241 Vilnius, Lithuania

ABSTRACT

Radicicol is a natural antibiotic that specifically inhibits chaperone Hsp90 activity and binds to its active site with nanomolar affinity. Radicicol has been widely used as a lead compound to generate synthetic analogs with reduced toxicity and increased stability that could be employed clinically. Here we present a detailed thermodynamic description of radicicol binding to human Hsp90 and yeast Hsc82 studied by isothermal titration calorimetry and thermal shift assay. Titrations as a function of pH showed a linked protonation event upon radicicol binding. The intrinsic binding constant and the thermodynamic parameters (including the enthalpy, entropy, and heat capacity) were determined for yeast Hsc82, and human alpha and beta Hsp90. Recent experimental evidence in literature shows that yeast Hsc82 has significant differences from human Hsp90 isozymes. Here we support this by demonstrating differences in radicicol binding thermodynamics to these proteins. The intrinsic enthalpy of radicicol binding to Hsc82 was -46.7 kJ/mol, to Hsp90alpha -70.7 kJ/mol, and to Hsp90beta was -66.8 kJ/mol. The enthalpies of binding were significantly different, while the intrinsic dissociation constants were quite similar,

ACCEPTED MANUSCRIPT

equal to 0.25, 0.04, and 0.15 nM, respectively. The structural features responsible for such large difference in binding enthalpy but small difference in the intrinsic binding Gibbs free energy are discussed.

KEYWORDS

Isothermal titration calorimetry; Thermal shift assay; ThermoFluor; Heat shock protein 90; Enthalpy

ACCEPTED MANUSCRIPT

ACCEPTED MANUSCRIPT

INTRODUCTION

Heat shock protein 90 (Hsp90) is a component of the cellular chaperone machinery[1; 2]. There are a number of recent developments in the understanding of the interesting and complex mechanism of Hsp90 action[3; 4; 5; 6; 7]. Hsp90 is over-expressed in cancer cells and Hsp90 inhibitors have shown selectivity for cancer cells. Therefore, small-molecule inhibitors are being developed as anticancer therapeutics[8; 9; 10; 11; 12].

Two groups of natural product inhibitors of Hsp90, based on geldanamycin (GM) and radicicol (RD) have been discovered that bind to the N-terminal domain at the active site ATP-binding pocket. Both natural compounds have been used as leads to develop compounds with desired pharmaceutical properties such as increased potency and reduced toxicity[1; 9]. RD is the more potent binder of the two. Radicicol, also known as monorden, was originally discovered as an antifungal substance of fungal origin in 1953[13] and is a specific Hsp90 inhibitor[14]. The co-crystal structures of radicicol bound to the Hsp90 N-terminal domains from various species have been determined, and they show numerous hydrogen bonds with the ATP-binding pocket of the N-terminal domain[15; 16]. As determined using isothermal titration calorimetry (ITC) full-length yeast Hsc82 binds radicicol with a K_d of 19 nM, and the N-terminal domain of yeast Hsc82 binds radicicol with a K_d of 2.7 nM[15].

Here, we determine the thermodynamics of RD binding to the N-terminal domain of human Hsp90 using a combination of ITC and thermal shift assay (TSA). Isothermal titration calorimetry fully characterizes the thermodynamics of the binding reaction, including not only the K_d (Gibbs free energy), but also the enthalpy, entropy, and heat capacity of binding[17; 18; 19; 20]. The full thermodynamic description of binding is important for structure-based drug development[18; 20]. The thermal shift assay[21], also known as differential scanning fluorimetry[22] and ThermoFluor®[23], is a high-throughput screening method for hit selection and the determination of the protein-ligand binding constants used in the pharmaceutical industry[24]. This biophysical technique can be applied to any protein-ligand non-covalent binding reaction, independent of whether the ligand stabilizes or destabilizes the protein upon binding[25]. In cases when there is a single binding event, the ITC and TSA results complement each other for increased precision of the measurements[26]. In addition, the method is useful for the

ACCEPTED MANUSCRIPT

characterization of protein stability in the presence of various excipients[27] and the optimization of conditions for protein crystallization[28].

We have redetermined radicicol binding thermodynamics to yeast Hsc82 and determined binding to human Hsp90 alpha and beta isozymes using ITC and TSA methods to estimate the binding affinity of very tight interactions. Furthermore, linked protonation effects were determined and dissected from intrinsic binding thermodynamics showing large differences in intrinsic enthalpies but small differences in the intrinsic Gibbs free energies of binding. Our findings support recent demonstrations [29; 30; 31; 32; 33] which show that Hsc82, used as a model and archetypical Hsp90 machine, shows differences in the mode of action compared to other family members.

Because the binding affinity is a combined function of the binding enthalpy and the binding entropy, improved affinity could result when any or both terms are designed to contribute more favorably to binding[34]. The enthalpy and heat capacity of binding correlate with structural parameters such as hydrogen bond formation and hydrophobic contacts more closely than the Gibbs free energy. Despite structural determination of radicicol binding to Hsc82, the thermodynamic characterization of the linked protonation reactions[35] and comparison with human Hsp90 α and β isoforms has been insufficiently detailed to understand the binding energetics.

ACCEPTED MANUSCRIPT

ACCEPTED MANUSCRIPT

RESULTS

Isothermal titration calorimetry of radicicol binding to Hsp90. The energetics of radicicol binding to various constructs of human Hsp90α and Hsp90β, and yeast Hsc82 was measured using ITC. Figure 1A shows a representative raw data titration of Hsp90αN with radicicol. The binding reaction is strongly exothermic. The first 12 peaks represent the heats of binding and heats of dilution whereas the small peaks after the 12th injection represent the heats of dilution. The binding of radicicol to Hsp90 was found to be stoichiometric under all conditions examined. Variation of the time between injections did not affect the observed enthalpy indicating that the binding measurements were done under reversible equilibrium binding conditions.

Figure 1B shows the integrated ITC curves of radicicol binding to Hsp90αN in two buffers, 50 mM sodium phosphate or 50 mM Tris, both at pH 7.5, and at 25 °C. Similarly, Figure 1C shows the integrated ITC curves of radicicol binding to yeast Hsc82F in the same two buffers. The enthalpies of binding are different in buffers of different ionization enthalpy. Therefore, one or more proton binding/release events are linked to radicicol binding for both human and yeast proteins. To determine the intrinsic thermodynamic parameters of binding, the proton binding energetics has to be dissected from the energetics of radicicol binding.

Figure 1D compares the integrated ITC curves of radicicol binding to the N-terminal domains of α and β Hsp90 isozymes with the full-length proteins. It was important to determine whether there is a difference in the binding thermodynamics to α and β Hsp90 isoforms, as both isozymes are present in the human body. The binding to the N-terminal ATP-binding domain of the protein is often studied using the Hsp90 protein construct lacking the middle and C-terminal domains. Therefore, it was also important to determine whether the N-terminal domain of both isozymes bind radicicol with the same energetics as the full-length native protein. Differences between radicicol binding to the N-terminal and full-length protein were negligible and within the experimental error of ITC measurements. Furthermore, the ITC experiments were performed as a function of buffer, pH, temperature, and the type of Hsp90/Hsc82 construct to dissect the thermodynamic parameters of binding from the linked protonation values. All of the Hsp90 and Hsc82 constructs tested exhibited the protonation event linked to radicicol binding. The observed enthalpies of binding showed a marked difference between the values obtained in the Tris and

ACCEPTED MANUSCRIPT

phosphate buffers in the alkaline pH region. Human and yeast proteins bound radicicol with significantly different observed enthalpies and K_ds. Table 1 shows the observed binding parameters of selected ITC runs. The enthalpies of buffer ionization were taken from reference [36].

A theoretical treatment demonstrating the use of ITC measurements to dissect proton linkage from ligand binding was given by Murphy and coworkers [37; 38; 39]. If a protein has a single ligand-binding site and a single proton uptake is linked to the binding process (i.e., a proton is taken from the buffer solution), then there are four linked processes described by the thermodynamic parameters labeled *F* in Figure 2, Panel A.

When ligand binding affects and shifts the pK_a of any ionizable group on a protein molecule, the binding and protonation events are linked. All thermodynamic parameters, such as the Gibbs free energies (or binding constants), enthalpies, entropies, and the heat capacities, are additive. As it takes energy to shift the pK_a, the binding constant of a ligand would be diminished at the pH at which the proton needs to be taken or given to the buffer. If ligand binding is linked to the binding of a single proton, then the observed binding constant (K_{obs}) and the intrinsic binding constant to the protonated protein form (K_{intr}) are related by:

$$K_{obs} = K \quad \frac{1+10^{pH-pK_a{}^b}}{1+10^{pH-pK_a{}^f}} \tag{1}$$

$K_a{}^b$ and $K_a{}^f$ are the proton dissociation constants from the liganded and unliganded protein, respectively. The change in the number of protons bound by the protein upon binding of the ligand (*n*) is the difference between the fractional saturation of protons in the liganded and free protein:

$$n = f_p{}^b - f_p{}^f = \frac{10^{pK_a{}^b - pH}}{1+10^{pK_a{}^b - pH}} - \frac{10^{pK_a{}^f - pH}}{1+10^{pK_a{}^f - pH}} \tag{2}$$

The value of *n* can be determined by ITC because it contributes to the observed binding enthalpy ($\Delta_b H_{obs}$):

$$\Delta_b H_{obs} = \Delta_b H + n\Delta_b H_{buffer} \tag{3}$$

ACCEPTED MANUSCRIPT

$\Delta_b H$ is the enthalpy that would be measured in a buffer that has an ionization enthalpy $\Delta_b H_{buffer}$ equal to zero. However, it is not equal to the intrinsic binding enthalpy. A series of observed enthalpies measured at constant pH in buffers with different ionization enthalpies (Figure 2B) plotted as a function of buffer ionization enthalpy will yield a slope equal to n and an intercept of $\Delta_b H$ (Figure 2C). The n values (Eq. (2)) plotted as a function of the pH are shown in Figure 2D. The data points are obtained from the slopes as shown in Figure 2C, whereas the line is fitted to Eq. (2) and yields a pK_a^f equal to 6.6. The enthalpies in Figure 2B are fitted using the same pK_a^f (6.6). The pK_a^b could not be determined and is greater than 11 because there is no return to $n = 0$ in the pH region that is accessible for binding measurements. The enthalpy of protonation of the ionizable group that is affected by radicicol binding in the Hsp90αN-radicicol complex was best fit by the value of -8.0 kJ×mol^{-1}. The intrinsic (buffer-independent) enthalpy of radicicol binding can be estimated from the relationship:

$$\Delta_b H_{obs} = \Delta_b H \quad + n\Delta_b H_{complex} + n\Delta_b H_{buffer} \qquad (4)$$

As no experimental conditions were found where radicicol would bind to the deprotonated protein form, it was not possible to determine the protonation enthalpy difference between the free and liganded forms of Hsp90.

Figure 3 shows the dependencies of the intrinsic binding enthalpies as a function of temperature. The slopes of the lines give the intrinsic heat capacities of radicicol binding to Hsp90. The heat capacity of radicicol binding to Hsp90αN is equal to approximately -620 J×mol^{-1}×K^{-1}. Table 2 lists the intrinsic thermodynamic parameters of radicicol binding to all tested Hsp90 protein constructs.

The binding of radicicol to Hsp90 is very tight, on the order of single-digit nanomolar or even tighter. Direct measurements by titrating Hsp90 with radicicol by ITC cannot estimate the binding constant because the curve is too steep, as previously discussed[40]. The c value ($c = C \times K_b$, C is the molar concentration of the protein, and K_b is the binding constant, when the binding stoichiometry is 1:1) for an ITC titration must be between 5 and 500. However, our ITC measurements were carried out using Hsp90 concentrations of at least 4 μM, and the binding constant of radicicol is expected to be approximately 2×10^{10} M^{-1} [40]. Thus, the c value is at least

ACCEPTED MANUSCRIPT

80,000, significantly above the value of 500 required for ITC. Therefore, different methods are required to measure the binding constant accurately in this pH region. This could be done by ITC using displacement titration of a weakly-binding ligand. However, this approach did not work well for radicicol[40]. The most precise results were obtained using the thermal shift assay.

Thermal shift assay of radicicol binding to Hsp90. The thermal shift assay measures the binding constant of a ligand by determining the increase in the melting temperature of the protein that is caused by the ligand [25; 26]. Protein unfolding is monitored using the intrinsic tryptophan fluorescence or the fluorescence of an extrinsic probe (such as 1,8-anilinonaphtalene sulfonate, ANS) upon increasing the temperature of the protein solution at a constant heating rate. Soluble single-domain globular proteins melt with a single transition that is affected by ligands. Full-length Hsp90 yields a complicated multi-domain melting transition profile. However, the N-terminal domain of Hsp90 yields a single transition that can be analyzed using the thermal shift assay.

Figure 4 shows ANS fluorescence curves as a function of temperature at two pH values (pH 7.0 in panel A and pH 10.0 in panel B) and several radicicol concentrations. The concentration of Hsp90αN was 10 μM. With no radicicol added, and when the pH is 7.0, there is a steep increase in fluorescence observed at approximately 50 °C. This increase is due to protein unfolding that exposes hydrophobic surfaces where ANS can bind and be excluded from quenching by the aqueous environment[41]. ANS actually binds using a combination of hydrophobic and ionic interactions but the ion pairs between the ANS sulfonate groups and the protein amino groups are not visible using fluorescence[42; 43]. When the radicicol concentration is greater than that of the protein, the melting temperature of Hsp90 is increased by more than 10 °C.

Protein melting temperatures were determined by fitting the protein melting curves (Figure 4) according to Eq. (5):

$$y(T) = y_{F,T_m} + m_F(T - T_m) + \frac{(y_{U,T_m} - y_{F,T_m}) + (m_U - m_F)(T - T_m)}{1 + e^{\Delta_U H_{T_m} + \Delta_U C_p \left(T - T_m\right) - T\left(\Delta_U S_{T_m} + \Delta_U C_p \ln T/T_m\right)/RT}} \quad (5)$$

ACCEPTED MANUSCRIPT

$y(T)$ is the calculated fluorescence as a function of temperature; y_{F,T_m} is the fluorescence of the probe bound to folded native protein before the transition at T_m; y_{U,T_m} is the fluorescence of the probe bound to the unfolded protein after the unfolding transition at T_m; m_F is the slope of the fluorescence dependence on temperature when the probe is bound to the native protein; m_U is the slope of the fluorescence dependence on temperature when the probe is bound to the unfolded protein; $\Delta_U H_{T_m}$ is the enthalpy of protein unfolding at T_m; $\Delta_U S_{T_m}$ is the entropy of protein unfolding at T_m; $\Delta_U C_p$ is the heat capacity of protein unfolding and is assumed to be temperature-independent over the temperature range studied; R is the universal gas constant; and T is the absolute temperature (Kelvin).

A number of transition curves at various concentrations of added ligand were determined and plotted as a function of the concentration of added ligand, yielding the melting temperature (T_m) dependencies as a function of the radicicol concentration (Figure 4C). The curves in Figure 4C were fit globally according to Eq. (6), yielding the pH dependencies of the binding constants.

$$L_t = (K_{U,T_m} - 1)\left(\frac{P_t}{2K_{U,T_m}} + \frac{1}{K_{b,T_m}}\right) = \left(e^{-\Delta_U H_{T_r} + \Delta_U C_p (T_m - T_r) - T_m \Delta_U S_{T_r} + \Delta_U C_p \ln (T_m/T_r) / RT_m} - 1\right) \times \left[\frac{P_t}{2} \frac{1}{e^{-\Delta_U H_{T_r} + \Delta_U C_p (T_m - T_r) - T_m \Delta_U S_{T_r} + \Delta_U C_p \ln (T_m/T_r) / RT_m}} + \frac{1}{e^{-\Delta_b H_{T_0} + \Delta_b C_p (T_m - T_0) - T_m \Delta_b S_{T_0} + \Delta_b C_p \ln (T_m/T_0) / RT_m}}\right] \quad (6)$$

L_t is the total concentration of added ligand, K_{U,T_m} is the protein unfolding equilibrium constant at T_m; P_t is the total protein concentration; K_{b,T_m} is the ligand binding constant at T_m; $\Delta_U H_{T_r}$ is the enthalpy of protein unfolding at T_r; T_r is the protein melting temperature when no ligand is added; $\Delta_U S_{T_r}$ is the entropy of protein unfolding at T_r; $\Delta_U C_p$ is the heat capacity of protein unfolding and is assumed to be temperature-independent over the temperature range studied; $\Delta_b H_{T_0}$ is the enthalpy of ligand binding at T_0; T_0 is the temperature at which the binding process is studied (usually 37 °C); $\Delta_b S_{T_0}$ is the entropy of ligand binding at T_0; and $\Delta_b C_p$ is the heat capacity of ligand binding and is assumed to be temperature-independent over the temperature range studied.

ACCEPTED MANUSCRIPT

The binding constant at the physiological temperature T_0 is determined using Eq. (7):

$$K_{b,T_0} = e^{-\Delta_b H_{T_0} - T_0 \Delta_b S_{T_0} / RT_0} \quad (7)$$

The radicicol dosing curves in Figure 4C show the greatest shift in T_m at pH 6.5, but the unliganded protein is most stable at pH 7.5. At pH 9.0, the shift is significantly smaller than near neutral pH, indicating a significant decrease in the binding constant.

To compare radicicol binding to the two human Hsp90 isoforms, we carried out a thermal shift assay at various pH values. Figure 5 compares selected fluorescence profiles at pH 7.0 for α and β Hsp90N. The melting temperature shift is greater for the alpha isozyme. A similar result is seen in Figure 5B, where the radicicol dosing curves are shown at pH 8.0 for the two isozymes. Therefore, both the ITC and thermal shift assays show stronger radicicol binding to the alpha isozyme rather than the beta isozyme.

Figure 6 shows the pH dependencies of the binding constants as determined using ITC and TSA. Both methods clearly show that the observed binding constant decreases at pH values greater than approximately 7.0. The line in Figure 6 is fitted using the pK_a^f of 6.6 and the K_{intr} of 2.5×10^{10} M^{-1}. At pH values below 8.5, the observed binding constant is determined correctly only using the TSA, and it is underestimated using ITC because the *c* value is above 500 (as described above).

Thermodynamics of radicicol binding to the Hsp90 and Hsc82 isozymes. After dissecting the proton linkage, the intrinsic thermodynamic parameters of radicicol binding to four recombinant human Hsp90 constructs are shown in Figure 7. All intrinsic thermodynamic parameters of radicicol binding, including binding to yeast Hsc82, are listed in Table 2. Most importantly, it appears that radicicol binds about 4-5 times more strongly to Hsp90α than to Hsp90β. Truncating the protein did not affect the binding constant significantly. However, it should be kept in mind that it was more difficult to determine the K_d for the full protein as the TSA method was not used due to the complicated unfolding T-curve. Therefore, the data are based solely on ITC comparisons at pH values where reliable ITC data could be obtained (i.e., pH 8.0-9.0).

ACCEPTED MANUSCRIPT

Dissection of the radicicol binding thermodynamics into their enthalpic and entropic contributions shows that radicicol-Hsp90 binding is driven by enthalpy and opposed by entropy. However, the entropic opposition accounts for approximately only 10% of the energy opposing binding. About 90% of the binding energy comes from the favorable enthalpic contribution. The thermodynamic parameters of binding to the full-length protein and the N-terminal domain are very similar. The difference is within the error of the measurements (Table 2).

The heat capacity change during radicicol-Hsp90 binding is approximately equal to -700±140 $J \times mol \times K^{-1}$. The slight difference between the N-terminal and full-length forms of Hsp90, and between the alpha and beta isoforms is most likely due to the error of the measurements. The negative heat capacity is often considered a signature of hydrophobic interactions, and the value is approximately of the expected magnitude for a molecule that has the MW of radicicol.

There is a small but statistically significant difference between the enthalpy and the Gibbs free energy of radicicol binding to Hsp90α and Hsp90β. The binding is slightly weaker to Hsp90β than to Hsp90α. This reduction in affinity is caused primarily by less favorable enthalpic rather than entropic contributions. The reduction in the favorable Gibbs free energy was approximately equal to 4 kJ/mol, whereas the reduction in the favorable exothermic enthalpy was approximately equal to 7 kJ/mol.

However, the binding of radicicol to yeast Hsc82N and yeast Hsc82F differed significantly from the binding to human Hsp90. The enthalpy of binding to the yeast forms of both protein constructs was less exothermic than was the binding to the human protein (Table 1). Full protonation linkage analysis determined that the enthalpy of protonation of an unknown protein group linked to radicicol binding was essentially the same as in both human isozymes indicating that the same residue is responsible for the linked protonation event.

However, the most striking difference between yeast and human isozymes is in the intrinsic enthalpy of binding. The enthalpy of radicicol binding to yeast Hsc82F was 20.1 kJ/mol less exothermic than Hsp90αF isozyme and 14.4 kJ/mol less exothermic than Hsp90βF isozyme. This large difference in enthalpies combined with relatively small difference in the intrinsic Gibbs free energies yields opposing contributions from the entropy of binding. It appears that

ACCEPTED MANUSCRIPT

radicicol binding to human Hsp90 isozymes is entropically opposed while binding to yeast Hsc82 is entropically favored process. However, overall enthalpic contribution to the binding reaction is significantly greater than the entropic contribution.

Despite the difficulties involved and the large number of ITC titrations required to carry out the full thermodynamic proton linkage analysis, it is important to dissect the linkage to obtain the intrinsic binding parameters of any ligand. The binding of radicicol to Hsp90 is a good example of a single binding-linked protonation event for which the thermodynamic characterization of binding would yield misleading results without the linkage analysis.

ACCEPTED MANUSCRIPT

ACCEPTED MANUSCRIPT

DISCUSSION

Radicicol is an important natural inhibitor of Hsp90 that has been used as a lead compound to design inhibitors for therapeutic purposes. It is now at preclinical development at the Memorial Sloan-Kettering Cancer Center[12]. Single amino acid mutations in Hsp90 may increase resistance to radicicol through an increased affinity of mutated Hsp90 to cochaperone Aha1[44] and are not related to change in radicicol affinity. Other mutants, however, directly affect radicicol binding affinity at the active site[16].

Radicicol binding to Hsc82 was characterized structurally by determining the structures of various protein constructs with radicicol using X-ray crystallography. A detailed mechanism of resistance to radicicol was recently determined for the fungus *Humicola fuscoatra*, which produces radicicol[5]. The Hsp90 from the fungus contains amino acid substitutions that reduce radicicol affinity but do not affect ATPase activity. However, despite detailed structural studies, we lacked a detailed energetic characterization of the interaction of radicicol with Hsp90. Various studies only use several ITC experiments and determine a limited number of association constants, without reporting the intrinsic binding enthalpies, entropies, and heat capacities.

To correlate the structural features of binding (such as the intermolecular van der Waals contacts, hydrogen bonds and presence of water molecules) with the energetics of binding one needs to carry out a detailed thermodynamic study of the binding reaction and to determine various dependencies (such as the pH-, buffer-, and temperature-dependencies). If there are any binding-linked protonation reactions, it is necessary to dissect their input to every thermodynamic parameter of the binding. Even after this analysis, it may not be possible to assign energetic parameters to all of the structural parameters. The binding reaction may contain a number of other linked events, such as any protein conformational changes that may occur upon ligand binding[45].

The dissection of linked protonation reactions and the application of two biophysical techniques, i.e., ITC and TSA, determined the K_d values of radicicol with Hsp90α to be approximately 0.04 nM, with Hsp90β to be approximately 0.15 nM, and with Hsc82 to be approximately 0.25 nM. These values are significantly tighter than determined previously using ITC[15] and without the

ACCEPTED MANUSCRIPT

dissection of the linked protonation reactions. This approach was more accurate than the displacement ITC experiments, as previously discussed.[40] The combination of ITC and TSA helps to determine ultra-tight binding constants by analyzing the pH-dependence (Figure 6). Interestingly, geldanamycin was shown to inhibit Hsp90α about 3-fold tighter than Hsp90β[46].

The main uncertainty of the TSA method is the precision of the enthalpy of Hsp90 protein unfolding. A 10% uncertainty in the value of unfolding enthalpy yields an uncertainty of the binding constant of ~2 fold[26]. The enthalpy of unfolding can be determined using several biophysical techniques such as DSC and acid-titration ITC[47; 48], and by fitting raw TSA curves or ligand-dosing curves[40]. The enthalpy of unfolding was accurately measured by all these methods only for the single-domain Hsp90N, but could not be done as precisely for the full-length multi-domain Hsp90 protein. Therefore, radicicol binding to Hsp90F was not determined by TSA. However, the binding constants for the full-length protein were shown to be the same as for the N-terminal Hsp90 domain by the ITC titrations at pH 8.0-9.0 and thus assumed to be the same at pH 7.0, where binding is too tight to be determined by ITC.

There were no such conditions found at high pH where there would be no linked protonation event. Therefore, it was not possible to determine the pK_a shift of the amino acid in Hsp90 responsible for the proton uptake at high pH. As the pK_a value was approximately 6.6, it is natural to assume that it is a histidine residue that binds a proton from aqueous solution upon radicicol binding (i.e., that a histidine residue is required to be protonated for the Hsp90 to bind radicicol).

However, there are no histidines in human Hsp90 in the proximity of the radicicol-binding site. Therefore, the linkage may be related to aspartic acid 93 (corresponding to D79 in yeast Hsc82), which is located in the immediate vicinity of the radicicol binding-site. We have constructed D93A and D93E mutants in order to test this possibility. However, both mutants did not express well or went to inclusion bodies indicating that the protein with such mutation has very different structure and stability. As a control, several other adjacent D mutants expressed and purified well. This indicates that human D93 is crucial for the protein. Radicicol binding measurements could not be carried out with these mutants.

ACCEPTED MANUSCRIPT

The enthalpy of protonation of an unknown group was determined to be equal to -8.0 kJ×mol^{-1}. This is too small for a histidine residue (about -29 kJ/mol) or phenolic group of radicicol (about -21 kJ/mol). However, the value is close to the enthalpy of Asp protonation which is equal to -5.6±1.6 kJ/mol (based on values determined at 25 °C as reviewed in[36]). Therefore, we consider it to be highly likely that Asp93 is responsible for the linked protonation effect. However, the certain identity of the amino acid remains to be determined.

Figure 8A shows the structural arrangement of important radicicol interactions bound to Hsc82 (PDB ID 1bgq). Radicicol forms hydrogen bonds only with Asp79 and several water molecules. Other direct contacts between radicicol and protein are identical for the three protein isoforms. Therefore, other amino acids are not shown. There is no crystal structure available in the PDB of radicicol bound to any human Hsp90 isozyme. Therefore, a computational model of human Hsp90α in the radicicol-bound form was constructed on the basis of the high-resolution (1.55Å) structure of human Hsp90α complexed with dihydroxyphenyl amide inhibitor (PDB code: 3EKO). First, the human Hsp90α structure (3EKO) was superimposed with the native and mutant yeast Hsc82 structures (PDB: 1BGQ and 2WER, respectively) that were solved with radicicol bound. Superposition of the structures revealed that the aromatic rings of the inhibitors superimposed very closely in all three structures. Therefore, we obtained the human Hsp90α complex with radicicol by simply substituting the dihydroxyphenyl amide inhibitor with radicicol from any of the superimposed yeast structures. The radicicol-bound Hsp90β model was obtained using the model of Hsp90α bound to radicicol, constructed as described above. The few side chains that differ between Hsp90α and Hsp90β were replaced in the Hsp90α structure and positioned automatically using SCWRL3[49]. Water molecules that occupied essentially the same position in the human X-ray structure (3EKO) and both yeast structures (1BGQ and 2WER) were retained in the models.

Figure 8 B and C compares the hydrogen bond arrangements in the vicinity of radicicol, Asp93 and Ser52 (Hsp90α) or Ala (Hsp90β) that are most likely to account for the difference in the radicicol binding energetics to the alpha and beta isoforms. There is only one amino acid (residue 52) that differs in the vicinity of the radicicol binding site. There is no direct contact between Ser or Ala and radicicol. However, as described previously [16], water molecules play a crucial role in

ACCEPTED MANUSCRIPT

mediating the radicicol-Hsp90 interaction. When radicicol binds to the alpha isozyme, Ser52 makes three additional contacts that cannot be formed with the beta isozyme (in which Ala lacks the OH group). These three additional hydrogen bonds are likely to be responsible for ~7 kJ/mol of the enthalpy and ~4 kJ/mol of the Gibbs free energy difference between the radicicol binding to the alpha and beta isozymes. The binding is enthalpically more favorable when the additional hydrogen bonds are formed.

However, the structure of radicicol – Hsc82 complex is very similar to Hsp90β, but the energetics of binding is significantly different. The enthalpy of radicicol binding to Hsc82 is 14.4 kJ/mol less exothermic than for Hsp90β. This difference could not be assigned to any obvious structural features of the protein-radicicol complex. Therefore, additional possibilities such as linked folding or conformational change reaction coupled with the binding reaction must be considered as the possible source of the significant difference in binding enthalpy.

Heat capacity changes were calculated using five published empirical relationships between changes in solvent-accessible surface area and ΔC_p to compare with experimentally measured values (Table 3). Calculated heat capacities were significantly smaller in their absolute values than the experimental ΔC_p values. This indicates a conformational change occurring during radicicol binding to the chaperone similarly to the conformational change occurring upon ATP binding[45].

Radicicol binding to Hsp90 is interesting in many respects regarding drug design. First, the binding reaction is very tight (i.e., it has a very favorable Gibbs free energy). Second, the binding reaction has a very favorable enthalpy of binding. Third, there are few direct contacts between Hsp90 and radicicol that could account for such a large binding energy. Fourth, water molecules play an essential role in the recognition and binding.

ACCEPTED MANUSCRIPT

MATERIALS AND METHODS

Materials. Radicicol was purchased from A.G. Scientific, Inc., dissolved in DMSO at 50 mM, and stored at -20 ºC. The concentration of radicicol was determined spectrophotometrically using an extinction coefficient of 14,700 $M^{-1}cm^{-1}$ in methanol at 265 nm[50]. Partial degradation of radicicol in DMSO solution occurred if stored over a month, especially in the presence of reductants. It was important to prepare fresh solutions for all measurements.

Hsp90 constructs. Hsp90αN – the N-terminal domain of alpha Hsp90. The gene encoding full-length human Hsp90α protein was purchased from RZPD, Deutsches Ressourcenzentrum für Genomforschung GmbH (Germany). For protein expression, the N-terminal fragment of the Hsp90α gene, corresponding to amino acids 3-241, was inserted into the pET-15b vector (Novagen, Madison, WI, USA) using the XhoI/BamHI restriction sites, thereby fusing a His_6 tag to the N-terminus of the protein.

Hsp90αF – Full length alpha Hsp90 was cloned and purified as previously described[51].

Hsp90βF – Full-length beta Hsp90 was cloned from the gene that was amplified from the pBAD24Hsp90beta vector (the kind gift of Dr. Dawid Walerych) using the primers 5'-GGGGGTCTAGACATATGCCTGAGGAAGTGC-3' and 5'-GCTAAGTGTCGACCTAATCGACTTCTTCCA-3'. This was then cloned using the NdeI and SalI restriction sites into the pET28b expression vector.

Hsp90βN – the N-terminal domain of beta Hsp90. The sequence coding for the N-domain (amino acid residues 1-239) of human Hsp90 beta was amplified from the same template using the same forward primer and the reverse primer 5'-CATAAGCTTTATCTTACTCTTCTTTCTCACC-3'. This was then cloned using the NdeI and HindIII restriction sites into the pET28b expression vector.

Yeast Hsc82F. The yeast (*S. cerevisiae*) Hsc82 gene was amplified from cDNA (the kind gift of Dr. Pawel Bieganowski) using the primers: 5'-CGGCACATATGGCTGGTGAAACTTTTGAAT-3' and 5'-

ACCEPTED MANUSCRIPT

GCCGGATCCTTAATCAACTTCTTCCATCTCGG-3'. This was then cloned using the NdeI and BamHI restriction sites into the pET28b expression vector.

Yeast Hsc82N. Sequence coding for the yeast Hsc82 N-terminal domain (amino acid residues 1-222) was amplified from the Hsc82 plasmid (pET28b) using the same forward primer and the reverse primer 5'-GCCGGATCCTTATTCTGGAATTGGAACTTCCTTTTC-3'. This was then cloned using the NdeI and BamHI restriction sites into the pET28b expression vector.

Protein expression and purification. His_6-tagged Hsp90αN protein was expressed in the *Escherichia coli* strain BL21 (DE3). The bacterial cultures were grown until an A_{550} of 0.5 – 0.8 was reached, and the expression was induced by the addition of 1 mM isopropyl-1-thio-β-D-galactopyranoside (final concentration). Protein was purified according to Richter et al. [52]. The cells were lysed by sonication, and the soluble protein was purified using a Ni-IDA affinity column, followed by an anion exchange chromatography column (Amersham Biosciences). The eluted protein was dialyzed into a storage buffer containing 20 mM Hepes (pH 7.5) and 50 mM NaCl. The purity of the Hsp90αN preparations was analyzed using SDS-PAGE and determined to be higher than 98%. The protein concentrations were determined by UV-VIS spectrophotometry and confirmed using the standard Bradford method. The protein stock solution was stored at -70 ºC.

Other proteins (except Hsp90αN and Hsp90αF) were expressed in the *E. coli* BL21 RIL strain (Stratagene). All proteins carried an N-terminal His_6-tag and were purified on His-selective HF resin (Sigma) according to a standard protocol, before being further purified on a Resource Q column (Biorad) in a 0.05-0.50 M KCl gradient. The proteins were dialyzed against buffer containing 25 mM Hepes, pH 7.5, 150 mM KCl and 10% glycerol, and frozen in liquid nitrogen.

Isothermal titration calorimetry. The protein solutions (2-5 μM) were loaded into the VP-ITC isothermal titration calorimeter (Microcal, Inc.) cell (approximately 2 ml, with an active cell volume of 1.4 ml). The titration syringe (250 μl) was filled with 20 - 50 (usually 40) μM ligand solution. Titrations were carried out using 25 injections of 10 μl each, injected at 3 to 4 minute intervals. The stirring speed was 260 rpm. Titrations were carried out at a constant temperature in the 13 – 37 ºC temperature range. The ligand solutions were prepared in the same buffer as the

ACCEPTED MANUSCRIPT

protein solutions, and contained the same concentration of DMSO (usually 0.5-1%). The total number of independent ITC titration experiments was 140. Variation of the protein concentration (within 1-10 μM range) or the time intervals between injections (within 3-5 min range) did not affect the measured enthalpies to an extent greater than the standard error.

Protein denaturation experiments. The thermal shift assay was performed using the iCycler iQ Real Time Detection System (Bio-Rad, Hercules, CA), a Corbett Rotor-Gene 6000 (QIAGEN Rotor-Gene Q), and the ISS PC1 spectrofluorimeter equipped with a temperature-controlled water bath. The temperature reproducibility was measured to be ±0.2 ºC. The protein concentrations were measured spectrophotometrically (ε_{280} (Hsp90αN) = 15,930 $M^{-1}cm^{-1}$). The protein concentration was usually 10 μM and the ligand concentrations varied from 0 to 200 μM. Universal buffer containing 50 mM sodium phosphate, 50 mM sodium acetate, 25 mM sodium borate, and 50 mM sodium chloride was usually used for the pH-dependence experiments of the protein denaturation. DMSO was added to make up 0.5-1% (v/v) of the solution in each measurement. Unfolding of the protein was monitored by measuring the fluorescence of the solvatochromic fluorescent dye Dapoxyl™ sulfonic acid sodium salt (iCycler) or ANS, both usually at 50 μM. The total volume of the reaction was 10 μl when using the iCycler or Corbett instruments and 3 ml for the ISS PC1 cuvette that was covered to prevent evaporation. Samples in the iCycler or Corbett instruments were overlaid with 2.5 μl of silicone oil DC 200. For this assay, 96-well iCycler iQ PCR plates were used. Samples in the ISS PC1 were excited with 380±5 nm UV light, and the ANS fluorescence emission was registered at 510±5 nm. The samples were heated at a rate of 1 ºC/min. The binding constants obtained by the thermal shift assay have standard error better than 1.6 fold. The greatest source of error is in the determination of the enthalpy of unfolding. The T_m is determined with ±0.2 °C standard error.

Structure analysis and calculation of ΔC_p. Solvent accessible surface areas were calculated using Naccess computer program[53]. The differences in surface areas upon radicicol binding were estimated by subtracting the areas in the presence and absence of radicicol in the structures of 1bgq (Hsc82N) and modeled Hsp90αN and Hsp90βN. Heat capacities were calculated using empirical equation relating it to changes in non-polar and polar solvent-accessible surface areas ($\Delta A_{non\text{-}polar}$ and ΔA_{polar} respectively):

ACCEPTED MANUSCRIPT

$$\Delta C_P = k_1 \Delta A_{non\text{-}polar} + k_2 \Delta A_{polar}$$

where k_1 and k_2 are empirical coefficients determined for several protein sets reviewed in[54].

ACKNOWLEDGMENTS

The project was supported in part by EEA and Norway Grants 2004-LT0019-IP-1EEE and the Lithuanian Government.

ACCEPTED MANUSCRIPT

ACCEPTED MANUSCRIPT

REFERENCES

1. Taldone, T., Sun, W. & Chiosis, G. (2009). Discovery and development of heat shock protein 90 inhibitors. *Bioorg Med Chem* **17**, 2225-35.
2. Wandinger, S. K., Richter, K. & Buchner, J. (2008). The Hsp90 chaperone machinery. *J Biol Chem* **283**, 18473-7.
3. Neckers, L., Mollapour, M. & Tsutsumi, S. (2009). The complex dance of the molecular chaperone Hsp90. *Trends Biochem Sci* **34**, 223-6.
4. Neckers, L., Tsutsumi, S. & Mollapour, M. (2009). Visualizing the twists and turns of a molecular chaperone. *Nat Struct Mol Biol* **16**, 235-6.
5. Mayer, M. P., Prodromou, C. & Frydman, J. (2009). The Hsp90 mosaic: a picture emerges. *Nat Struct Mol Biol* **16**, 2-6.
6. Walerych, D., Olszewski, M. B., Gutkowska, M., Helwak, A., Zylicz, M. & Zylicz, A. (2009). Hsp70 molecular chaperones are required to support p53 tumor suppressor activity under stress conditions. *Oncogene* **28**, 4284-94.
7. Banz, V. M., Medova, M., Keogh, A., Furer, C., Zimmer, Y., Candinas, D. & Stroka, D. (2009). Hsp90 transcriptionally and post-translationally regulates the expression of NDRG1 and maintains the stability of its modifying kinase GSK3beta. *Biochim Biophys Acta* **1793**, 1597-603.
8. van Montfort, R. L. & Workman, P. (2009). Structure-based design of molecular cancer therapeutics. *Trends Biotechnol* **27**, 315-28.
9. Sharp, S. Y., Boxall, K., Rowlands, M., Prodromou, C., Roe, S. M., Maloney, A., Powers, M., Clarke, P. A., Box, G., Sanderson, S., Patterson, L., Matthews, T. P., Cheung, K. M., Ball, K., Hayes, A., Raynaud, F., Marais, R., Pearl, L., Eccles, S., Aherne, W., McDonald, E. & Workman, P. (2007). In vitro biological characterization of a novel, synthetic diaryl pyrazole resorcinol class of heat shock protein 90 inhibitors. *Cancer Res* **67**, 2206-16.
10. Sgobba, M. & Rastelli, G. (2009). Structure-based and in silico design of Hsp90 inhibitors. *ChemMedChem* **4**, 1399-409.
11. Zuehlke, A. & Johnson, J. L. (2010). Hsp90 and co-chaperones twist the functions of diverse client proteins. *Biopolymers* **93**, 211-7.
12. Fukuyo, Y., Hunt, C. R. & Horikoshi, N. (2009). Geldanamycin and its anti-cancer activities. *Cancer Lett*.
13. Delmotte, P. & Delmotte-Plaque, J. (1953). A new antifungal substance of fungal origin. *Nature* **171**, 344.
14. Schulte, T. W., Akinaga, S., Soga, S., Sullivan, W., Stensgard, B., Toft, D. & Neckers, L. M. (1998). Antibiotic radicicol binds to the N-terminal domain of Hsp90 and shares important biologic activities with geldanamycin. *Cell Stress Chaperones* **3**, 100-8.
15. Roe, S. M., Prodromou, C., O'Brien, R., Ladbury, J. E., Piper, P. W. & Pearl, L. H. (1999). Structural basis for inhibition of the Hsp90 molecular chaperone by the antitumor antibiotics radicicol and geldanamycin. *J Med Chem* **42**, 260-6.
16. Prodromou, C., Nuttall, J. M., Millson, S. H., Roe, S. M., Sim, T. S., Tan, D., Workman, P., Pearl, L. H. & Piper, P. W. (2009). Structural Basis of the Radicicol Resistance Displayed by a Fungal Hsp90. *ACS Chem Biol* **4**, 289-97.
17. Nilapwar, S., Williams, E., Fu, C., Prodromou, C., Pearl, L. H., Williams, M. A. & Ladbury, J. E. (2009). Structural-thermodynamic relationships of interactions in the N-terminal ATP-binding domain of Hsp90. *J Mol Biol* **392**, 923-36.

ACCEPTED MANUSCRIPT

18. Velazquez Campoy, A. & Freire, E. (2005). ITC in the post-genomic era...? Priceless. *Biophys Chem* **115**, 115-24.
19. Velazquez-Campoy, A., Ohtaka, H., Nezami, A., Muzammil, S. & Freire, E. (2004). Isothermal titration calorimetry. *Curr Protoc Cell Biol* **Chapter 17**, Unit 17 8.
20. Freire, E. (2004). Isothermal titration calorimetry: controlling binding forces in lead optimization. *Drug Discov. Today: Technologies* **1**, 295-299.
21. Lo, M. C., Aulabaugh, A., Jin, G., Cowling, R., Bard, J., Malamas, M. & Ellestad, G. (2004). Evaluation of fluorescence-based thermal shift assays for hit identification in drug discovery. *Anal. Biochem.* **332**, 153-9.
22. Niesen, F. H., Berglund, H. & Vedadi, M. (2007). The use of differential scanning fluorimetry to detect ligand interactions that promote protein stability. *Nat Protoc* **2**, 2212-21.
23. Pantoliano, M. W., Petrella, E. C., Kwasnoski, J. D., Lobanov, V. S., Myslik, J., Graf, E., Carver, T., Asel, E., Springer, B. A., Lane, P. & Salemme, F. R. (2001). High-density miniaturized thermal shift assays as a general strategy for drug discovery. *J. Biomol. Screen.* **6**, 429-40.
24. Todd, M. J. & Salemme, F. R. (2003). Direct Binding Assays for Pharma Screening. *Genetic Eng. News* **23**, 28-29.
25. Cimmperman, P., Baranauskiene, L., Jachimoviciute, S., Jachno, J., Torresan, J., Michailoviene, V., Matuliene, J., Sereikaite, J., Bumelis, V. & Matulis, D. (2008). A quantitative model of thermal stabilization and destabilization of proteins by ligands. *Biophys J* **95**, 3222-3231.
26. Matulis, D., Kranz, J. K., Salemme, F. R. & Todd, M. J. (2005). Thermodynamic stability of carbonic anhydrase: measurements of binding affinity and stoichiometry using ThermoFluor. *Biochemistry* **44**, 5258-66.
27. Mezzasalma, T. M., Kranz, J. K., Chan, W., Struble, G. T., Schalk-Hihi, C., Deckman, I. C., Springer, B. A. & Todd, M. J. (2007). Enhancing recombinant protein quality and yield by protein stability profiling. *J. Biomol. Screen.* **12**, 418-428.
28. Ericsson, U. B., Hallberg, B. M., Detitta, G. T., Dekker, N. & Nordlund, P. (2006). Thermofluor-based high-throughput stability optimization of proteins for structural studies. *Anal. Biochem.* **357**, 289-298.
29. Krukenberg, K. A., Bottcher, U. M., Southworth, D. R. & Agard, D. A. (2009). Grp94, the endoplasmic reticulum Hsp90, has a similar solution conformation to cytosolic Hsp90 in the absence of nucleotide. *Protein Sci* **18**, 1815-27.
30. Vaughan, C. K., Piper, P. W., Pearl, L. H. & Prodromou, C. (2009). A common conformationally coupled ATPase mechanism for yeast and human cytoplasmic HSP90s. *Febs J* **276**, 199-209.
31. Pearl, L. H. & Prodromou, C. (2006). Structure and mechanism of the hsp90 molecular chaperone machinery. *Annu Rev Biochem* **75**, 271-94.
32. Mickler, M., Hessling, M., Ratzke, C., Buchner, J. & Hugel, T. (2009). The large conformational changes of Hsp90 are only weakly coupled to ATP hydrolysis. *Nat Struct Mol Biol* **16**, 281-6.
33. Hessling, M., Richter, K. & Buchner, J. (2009). Dissection of the ATP-induced conformational cycle of the molecular chaperone Hsp90. *Nat Struct Mol Biol* **16**, 287-93.
34. Freire, E. (2008). Do enthalpy and entropy distinguish first in class from best in class? *Drug Discov Today* **13**, 869-74.
35. Doyle, M. L., Louie, G., Dal Monte, P. R. & Sokoloski, T. D. (1995). Tight binding affinities determined from thermodynamic linkage to protons by titration calorimetry. *Methods Enzymol* **259**, 183-94.
36. Christensen, J. J., Hansen, L. D. & Izatt, R. M. (1976). *Handbook of Proton Ionizations Heats*, Wiley-Interscience.

ACCEPTED MANUSCRIPT

37. Baker, B. M. & Murphy, K. P. (1996). Evaluation of linked protonation effects in protein binding reactions using isothermal titration calorimetry. *Biophysical Journal* **71(4)**, 2049-55.
38. Baker, B. M. & Murphy, K. P. (1997). Dissecting the energetics of a protein-protein interaction: the binding of ovomucoid third domain to elastase. *Journal of Molecular Biology* **268(2)**, 557-69.
39. Bradshaw, J. M. & Waksman, G. (1998). Calorimetric investigation of proton linkage by monitoring both the enthalpy and association constant of binding: application to the interaction of the Src SH2 domain with a high-affinity tyrosyl phosphopeptide. *Biochemistry* **37**, 15400-7.
40. Zubriene, A., Matuliene, J., Baranauskiene, L., Jachno, J., Torresan, J., Michailoviene, V., Cimmperman, P. & Matulis, D. (2009). Measurement of Nanomolar Dissociation Constants by Titration Calorimetry and Thermal Shift Assay - Radicicol Binding to Hsp90 and Ethoxzolamide Binding to CAII. *Int J Mol Sci* **10**, 2662-2680.
41. Anderson, S. R. & Weber, G. (1969). Fluorescence polarization of the complexes of 1-anilino-8-naphthalenesulfonate with bovine serum albumin. Evidence for preferential orientation of the ligand. *Biochemistry* **8**, 371-7.
42. Matulis, D., Baumann, C. G., Bloomfield, V. A. & Lovrien, R. E. (1999). 1-anilino-8-naphthalene sulfonate as a protein conformational tightening agent. *Biopolymers* **49**, 451-8.
43. Matulis, D. & Lovrien, R. (1998). 1-Anilino-8-naphthalene sulfonate anion-protein binding depends primarily on ion pair formation. *Biophys J* **74**, 422-9.
44. Zurawska, A., Urbanski, J., Matuliene, J., Baraniak, J., Klejman, M. P., Filipek, S., Matulis, D. & Bieganowski, P. (2010). Mutations that increase both Hsp90 ATPase activity in vitro and Hsp90 drug resistance in vivo. *Biochim Biophys Acta* **1803**, 575-83.
45. Dehner, A., Furrer, J., Richter, K., Schuster, I., Buchner, J. & Kessler, H. (2003). NMR chemical shift perturbation study of the N-terminal domain of Hsp90 upon binding of ADP, AMP-PNP, geldanamycin, and radicicol. *Chembiochem* **4**, 870-7.
46. Gooljarsingh, L. T., Fernandes, C., Yan, K., Zhang, H., Grooms, M., Johanson, K., Sinnamon, R. H., Kirkpatrick, R. B., Kerrigan, J., Lewis, T., Arnone, M., King, A. J., Lai, Z., Copeland, R. A. & Tummino, P. J. (2006). A biochemical rationale for the anticancer effects of Hsp90 inhibitors: Slow, tight binding inhibition by geldanamycin and its analogues. *Proc Natl Acad Sci U S A* **103**, 7625-30.
47. Nakamura, S. & Kidokoro, S. (2004). Isothermal acid-titration calorimetry for evaluating the pH dependence of protein stability. *Biophys Chem* **109**, 229-49.
48. Baranauskiene, L., Matuliene, J. & Matulis, D. (2008). Determination of the thermodynamics of carbonic anhydrase acid-unfolding by titration calorimetry. *J Biochem Biophys Methods* **70**, 1043-7.
49. Canutescu, A. A., Shelenkov, A. A. & Dunbrack, R. L., Jr. (2003). A graph-theory algorithm for rapid protein side-chain prediction. *Protein Sci* **12**, 2001-14.
50. Sigg, H. P. & Loeffler, W. (1969). Production of radicicol, USA.
51. Cikotiene, I., Kazlauskas, E., Matuliene, J., Michailoviene, V., Torresan, J., Jachno, J. & Matulis, D. (2009). 5-Aryl-4-(5-substituted-2,4-dihydroxyphenyl)-1,2,3-thiadiazoles as inhibitors of Hsp90 chaperone. *Bioorg Med Chem Lett* **19**, 1089-92.
52. Richter, K., Muschler, P., Hainzl, O. & Buchner, J. (2001). Coordinated ATP hydrolysis by the Hsp90 dimer. *J Biol Chem* **276**, 33689-96.
53. Hubbard, S. J. & Thornton, J. M. D. o. B. a. M. B. U. C. L. (1993). 'NACCESS', Computer Program.
54. Prabhu, N. V. & Sharp, K. A. (2005). Heat capacity in proteins. *Annu Rev Phys Chem* **56**, 521-48.

ACCEPTED MANUSCRIPT

TABLES

Table 1. Representative ITC data for the binding of radicicol to recombinant human and yeast Hsp90 protein constructs as a function of pH, temperature, and buffer ionization enthalpy.

Construct	Temp., °C	*pH*	Buffer	$\Delta_{ioniz}H_{buf}$ [a]	$\Delta_b H_{obs}$ [a]	K_d, nM
Hsp90αN	13	7.5	Pi[b]	7.4	-63.5	1.3
	25	7.5	Pi	5.1	-72.9	0.15
	37	7.5	Pi	2.9	-81.2	0.47
	25	5.5	Tris	47.5	-71.1	0.24
	25	6.0	Tris	47.5	-59.3	0.14
	25	6.5	Tris	47.5	-55.5	0.34
	25	7.0	Tris	47.5	-48.7	0.03
	25	7.5	Tris	47.5	-44.8	0.91
	25	8.0	Tris	47.5	-40.7	1.4
	25	8.5	Tris	47.5	-37.7	7.4
	25	9.0	Tris	47.5	-35.9	73.2
	25	6.0	Pi	5.1	-68.7	0.29
	25	8.5	Pi	5.1	-72.8	8.6
Hsp90αF	13	7.5	Pi	7.4	-55.5	1.06
	25	7.5	Pi	5.1	-68.6	0.32
	37	7.5	Pi	2.9	-77.4	0.43
	25	6.0	Tris	47.5	-51.1	1.23
	25	7.5	Tris	47.5	-40.7	0.21
	25	8.5	Tris	47.5	-35.6	5.8
	25	6.0	Pi	5.1	-69.0	2.0
	25	8.5	Pi	5.1	-62.3	4.0
Hsp90βN	13	7.5	Pi	7.4	-56.3	2.9
	25	7.5	Pi	5.1	-62.7	0.5
	37	7.5	Pi	2.9	-75.3	3.1
	25	6.0	Tris	47.5	-55.2	0.55
	25	7.5	Tris	47.5	-35.7	0.34
	25	8.5	Tris	47.5	-30.9	10.06
	25	6.0	Pi	5.1	-66.9	0.07
	25	8.5	Pi	5.1	-60.3	5.91
Hsp90αN	37	7.5	Hepes	21.6	-70.4	0.6
Hsp90αF	37	7.5	Hepes	21.6	-69.1	0.59
Hsp90βN	37	7.5	Hepes	21.6	-59.3	2.0
Hsp90βF	37	7.5	Hepes	21.6	-59.0	3.0
yeastHsc82N	37	7.5	Hepes	21.6	-52.5	9.6
yeastHsc82F	37	7.5	Hepes	21.6	-53.2	26.0
	25	7.5	Tris	47.5	-18.5	2.38
	13	7.5	Pi	7.4	-42.6	1.46
	25	7.5	Pi	5.1	-48.8	7.69
	37	7.5	Pi	2.9	-57.6	13.9

ACCEPTED MANUSCRIPT

a: units in kJ×mol^{-1}; b: Pi is phosphate buffer. The standard deviations were 3 to 5 kJ×mol^{-1} for the enthalpy and up to 1.6 fold for the K_d, especially when the binding was too tight to measure accurately using ITC.

ACCEPTED MANUSCRIPT

ACCEPTED MANUSCRIPT

Table 2. The intrinsic thermodynamic parameters of radicicol binding to Hsp90 at 25 °C.

Protein	K_d, nM	$\Delta_b H_{intr}$, kJ×mol^{-1}	$\Delta_b G_{intr}$, kJ×mol^{-1}	$T\Delta_b S_{intr}$, kJ×mol^{-1}	$\Delta_b S_{intr}$, J×mol^{-1}×K^{-1}	$\Delta_b C_p$, J×mol^{-1}×K^{-1}
Hsp90αN	0.04	-70.7	-59.4	-11.4	-38	-620
Hsp90αF	0.04	-66.8	-59.4	-7.5	-25	-860
Hsp90βN	0.15	-60.6	-56.1	-4.6	-15	-760
Hsp90βF	0.15	-61.1	-56.1	-5.0	-17	N.D
Hsc82F	0.25	-46.7	-54.8	8.1	27.1	-620
Uncertainties	±1.6-fold	±4	±2.6	±4.7	±16	±140

ACCEPTED MANUSCRIPT

ACCEPTED MANUSCRIPT

Table 3. Experimental and calculated ΔC_p values for the binding of radicicol to Hsp90α, Hsp90β, and Hsc82. The ΔC_p values were calculated using area coefficients reviewed in[54].

Solvent accessible surface area and heat capacity difference upon binding	Hsp90α	Hsp90β	Hsc82
$\Delta A_{nonpolar\text{-}calculated}$, Å^2	-191	-193	-182,4
$\Delta A_{polar\text{-}calculated}$, Å^2	-58,6	-57,4	-71,9
$\Delta C_{p\text{-}experimental}$, J×mol^{-1}×K^{-1}	**-620**	**-760**	**-620**
$\Delta C_{p\text{-}calc\text{-}Spolar}$, J×mol^{-1}×K^{-1}	-221	-225	-202
$\Delta C_{p\text{-}calc\text{-}Murphy\text{-}Freire}$, J×mol^{-1}×K^{-1}	-295	-300	-265
$\Delta C_{p\text{-}calc\text{-}Meyers}$, J×mol^{-1}×K^{-1}	-201	-204	-186
$\Delta C_{p\text{-}calc\text{-}Makhatadze\text{-}Privalov}$, J×mol^{-1}×K^{-1}	-357	-363	-327
$\Delta C_{p\text{-}calc\text{-}Robertson\text{-}Murphy}$, J×mol^{-1}×K^{-1}	-157	-157	-158

ACCEPTED MANUSCRIPT

ACCEPTED MANUSCRIPT

FIGURE LEGENDS

Figure 1. Representative isothermal titration calorimetry curves of radicicol binding to various human and yeast Hsp90 family member protein constructs. Panel A. The raw data curves of radicicol binding to Hsp90αN in 50 mM sodium phosphate, pH 7.5, at 25 °C. Insert shows the chemical structure of radicicol. Panel B. The integrated ITC data curves of radicicol binding to Hsp90αN in two buffers: ■ – in sodium phosphate, and Δ – in Tris chloride buffer, both at pH 7.5 and 25 °C. Note that the observed enthalpy of binding is significantly more exothermic in phosphate than in Tris buffer. Panel C. The integrated ITC data curves of radicicol binding to yeast Hsc82 in the same conditions. Note that the observed enthalpies are significantly different from Hsp90αN. Panel D. Integrated ITC data curves of radicicol binding to various constructs of Hsp90 : ▲ – Hsp90αN, Δ – Hsp90αF, ■ – Hsp90βN, and □ – Hsp90βF. Solid lines show curve fits for the N-terminal Hsp90 while the dashed lines show curve fits for the full-length Hsp90. Differences between the N-terminal and full-length protein binding were within the experimental error. All of the tested constructs bound radicicol stoichiometrically. The intrinsic parameters of radicicol binding to various Hsp90 constructs and isozymes are summarized in Table 2.

Figure 2. Demonstration of the linked protonation event observed upon radicicol binding to Hsp90αN. Panel A. Schematic representation of the linked protonation events. Here F_b^f represents ligand binding to unprotonated protein, F_b^p represents ligand binding to protonated protein, F_p^f represents proton binding to free (unliganded) protein, and F_p^b represents proton binding to ligand-bound protein. Panel B. The observed enthalpies as a function of pH in two buffers: Δ – phosphate, and ■ – tris. The data points are the enthalpies that were observed experimentally using ITC, and the lines are fitted to the single binding-linked protonation model, Eq. (4). Panel C. The observed enthalpies as a function of the buffer deprotonation enthalpy at various temperatures: ◆ – 13 °C, □ – 25 °C, and ▲ – 37 °C. The data points are the experimentally-observed enthalpies, and the trendlines are linear fits. Their slopes are equal to the binding-linked protonation events. There was little change of *n* as a function of temperature.

ACCEPTED MANUSCRIPT

The zero intercepts of the lines are equal to the buffer-independent binding enthalpies. The enthalpies are not intrinsic binding enthalpies because they contain the heats of protonation of unknown protein functional groups. Panel D. The number of linked protonation events (n), obtained from the slopes of the lines in Panel C as a function of pH. The line is fitted to the single binding-linked protonation model, Eq. (4). The midpoint of the curve occurring around pH 6.6 indicates the existence of a functional group on the protein that has a pK_a ~6.6. Radicicol binds to the protonated form of the protein. Therefore the protein must bind a proton to bind radicicol.

Figure 3. Intrinsic binding enthalpies obtained after accounting for the linked protonation event as a function of temperature for radicicol binding to various proteins. Panel A: ■ – Hsp90αN, and ▲ – Hsp90αF. Panel B: ■ – Hsp90αN, and ● – Hsp90βN. The slopes are linear fits to the experimental data and are equal to the intrinsic heat capacities of radicicol binding. The intrinsic binding parameters are summarized in Table 2.

Figure 4. Radicicol binding to Hsp90αN determined from the thermal shift assay. Raw data at pH 7.0 (Panel A) and pH 10.0 (Panel B). The Hsp90 thermal denaturation transitions (T_m) were increasingly shifted upwards as the concentrations of radicicol increased: ■ – 0 μM, × – 40 μM, Δ – 80 μM, and ◆ – 160 μM. Note that both the unliganded and liganded forms of Hsp90αN were destabilized at pH 10.0 and also made the relative T_m shift smaller than at pH 7.0. Panel C. The T_m data from the thermal shift assay as a function of the concentration of added radicicol at various pH values. The data points are obtained from the raw data as in Panels A, B, and the lines are fitted according to the model, Eq. (6). Note that the protein is most stable at pH 7.5-9.0, but the T_m shift caused by the ligand is greatest at pH 6.5. The leftmost data point is obtained when no radicicol is added.

ACCEPTED MANUSCRIPT

Figure 5. Radicicol binding to the Hsp90 α and β isoforms at pH 8.0 from the thermal shift assay. Panel A. The raw data. Filled symbols - Hsp90αN, open symbols - Hsp90βN. The triangles show the melting curves in the absence of added radicicol, whereas the squares show the protein melting curves after 20 μM radicicol is added. Panel B. The dependence of the melting temperature of Hsp90αN (■) and Hsp90βN (▲) on the concentration of radicicol. The melting temperature shift is greater for the α than the β isozyme. Analysis of the data shows that the binding constant is greater for the α than the β isozyme.

Figure 6. The observed binding constants of the interaction of radicicol with Hsp90αN obtained using three experimental approaches: Δ – isothermal titration calorimetry in phosphate buffer, ■ – isothermal titration calorimetry in Tris buffer, and × – the thermal shift assay, all at 25 °C. The line is fitted according to Eq. (1) for a linked protonation event using $pK_a^f = 6.6$. The pK_a^b is somewhere greater than 11, but the exact value is unknown. There is a clear decrease in the binding strength at higher pH. The dashed line shows the upper limit of accurate K_b determination by ITC (where the c value ($c = C \times K_b$) is 500). TSA provides more accurate values at low pH than does ITC.

Figure 7. The intrinsic thermodynamic parameters (squares – enthalpies, triangles – entropies, and circles – Gibbs free energies) of radicicol binding to various proteins as a function of temperature. Panel A: Hsp90αN (filled symbols) and Hsp90αF (open symbols). Panel B: Hsp90αN (filled symbols) and Hsp90βN (open symbols). The intrinsic binding constants and the Gibbs free energies were essentially indistinguishable for the two Hsp90α constructs (Panel A). Therefore, $\Delta_b G$ is shown as a single line for both constructs.

Figure 8. A structural model of radicicol binding to Hsp90. Panel A. Experimental crystal sctructure of radicicol bound to the yeast Hsc82 (pdb ID 1bgq). Panels B and C. Computational models of radicicol bound to the human Hsp90α (Panel B) and Hsp90β (Panel C), prepared as

ACCEPTED MANUSCRIPT

explained in the text. The human Hsp90 α and β isozymes differ only by one amino acid (position 52 in α) in the vicinity of radicicol binding site, i.e., Ser in α and Ala in β. The serine OH group can make three additional hydrogen bonds that cannot be formed in the beta isozyme, where the serine is replaced with alanine. This is essentially the only difference between two modeled structures, and is therefore likely to be responsible for the differences in the binding Gibbs free energy and enthalpy. Yeast Hsc82 contains Ala in the structurally equivalent position 38 (as in human Hsp90β).

ACCEPTED MANUSCRIPT

ACCEPTED MANUSCRIPT

FIGURES

Figure 1. Panels A and B

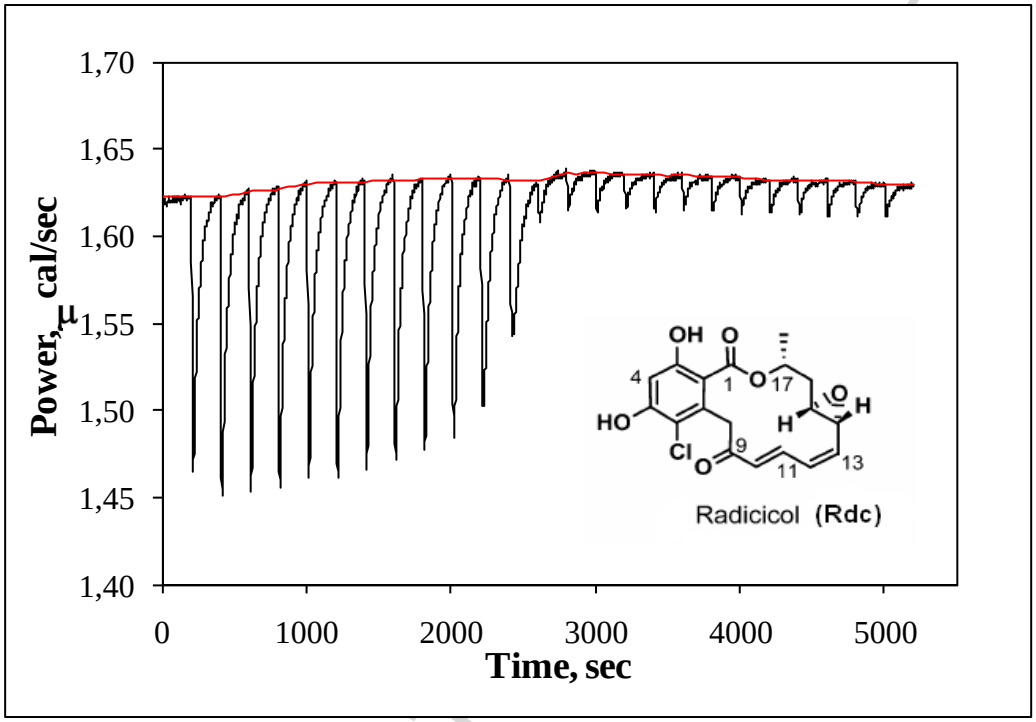

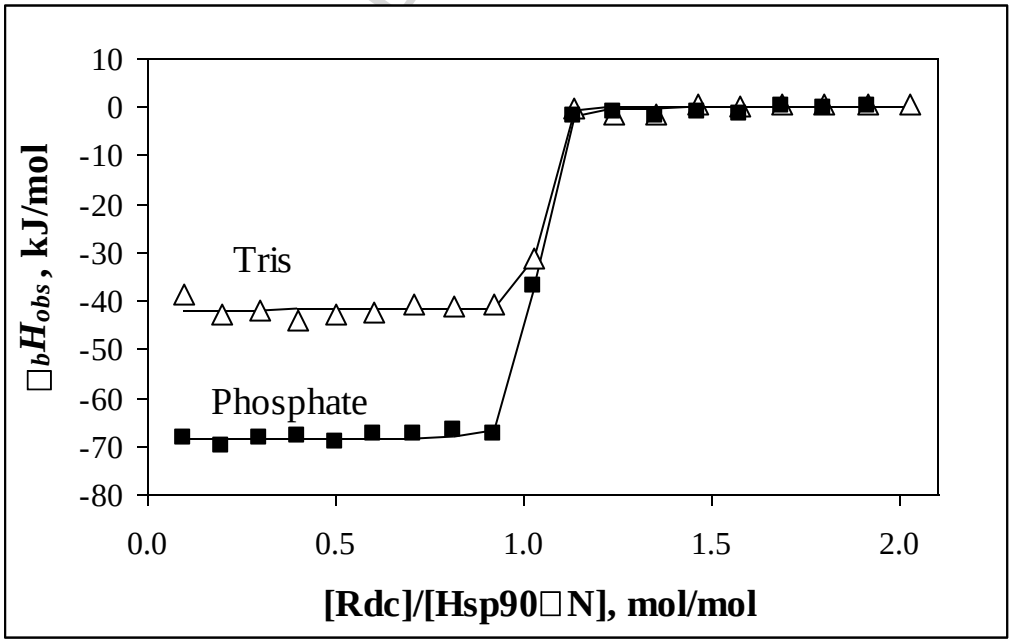

ACCEPTED MANUSCRIPT

Figure 1. Panels C and D

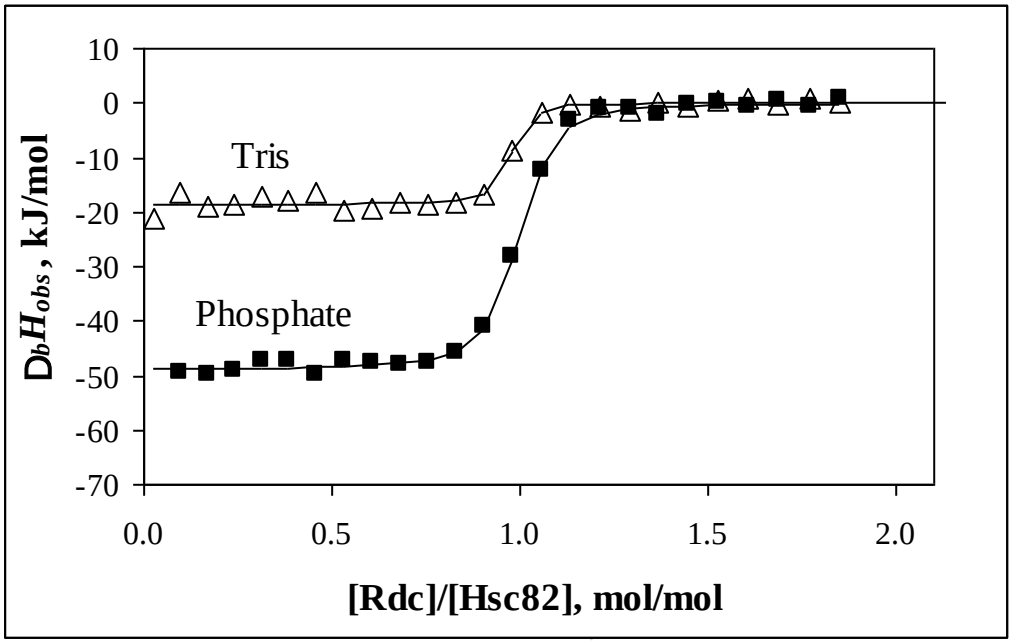

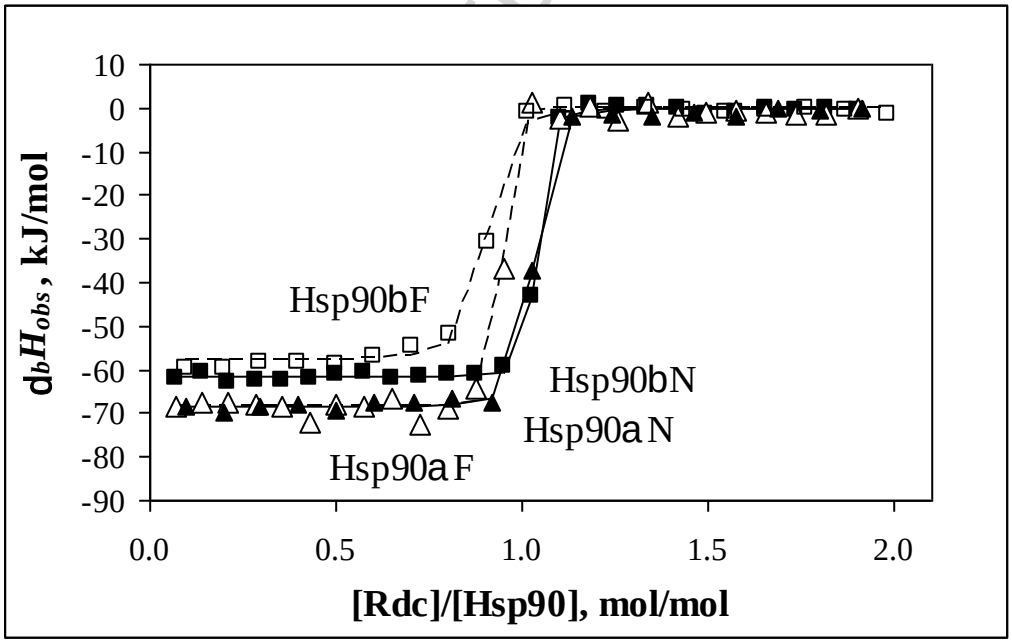

ACCEPTED MANUSCRIPT

Figure 2. Panel A:

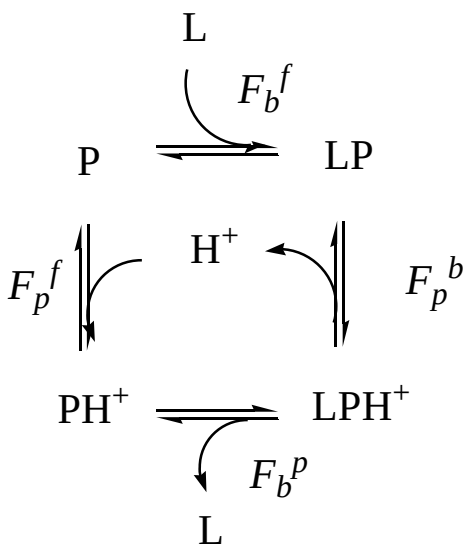

Figure 2, Panel B:

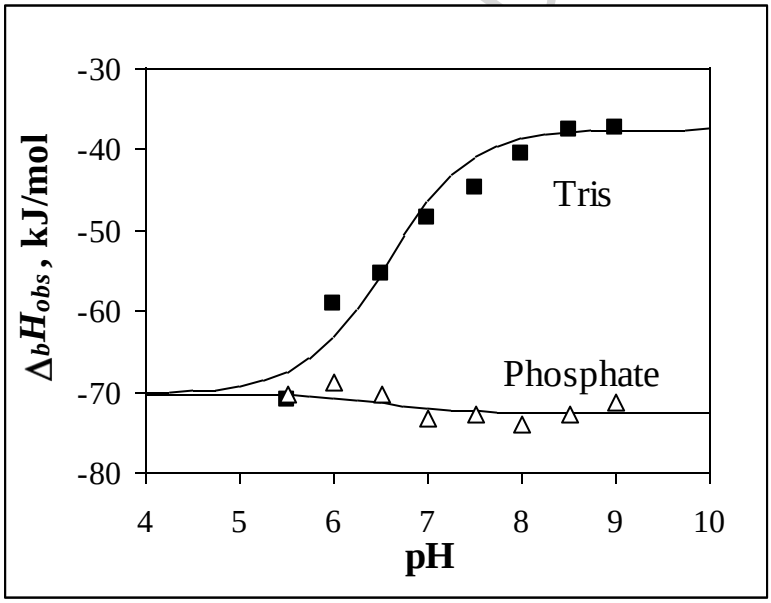

ACCEPTED MANUSCRIPT

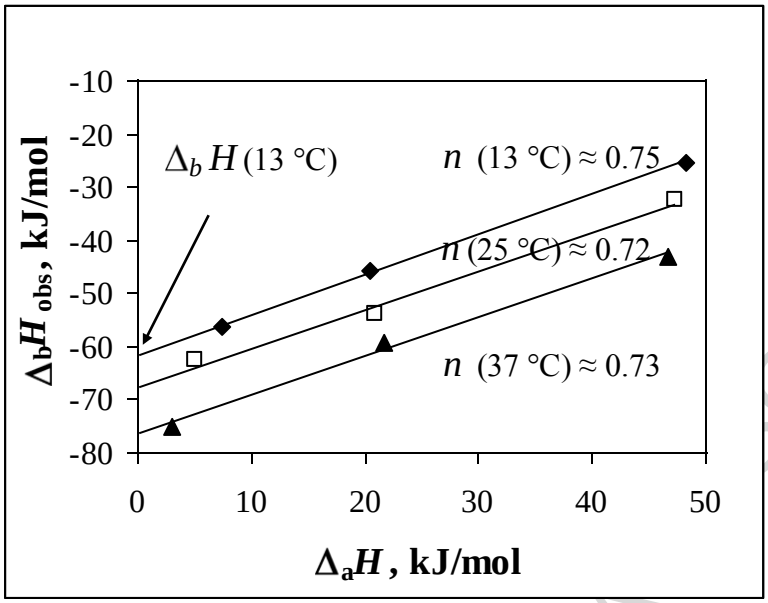

Figure 2. Panel C

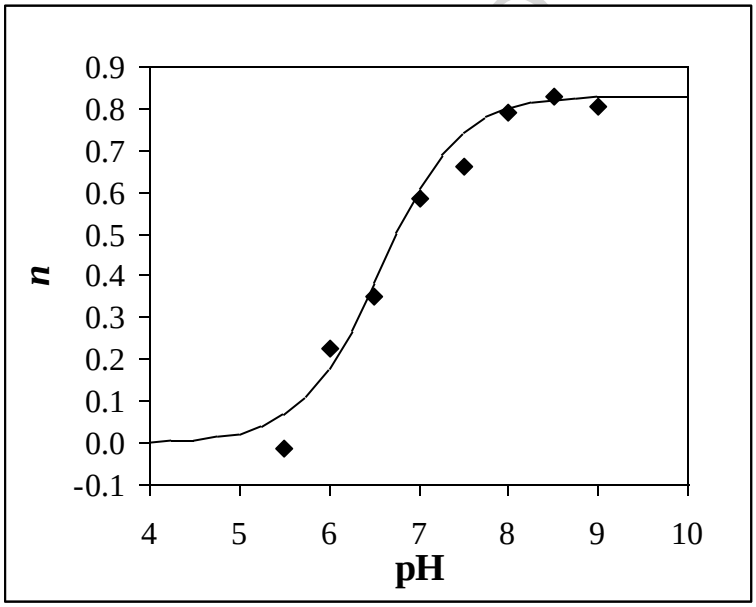

Figure 2. Panel D

ACCEPTED MANUSCRIPT

Figure 3. Panels A and B

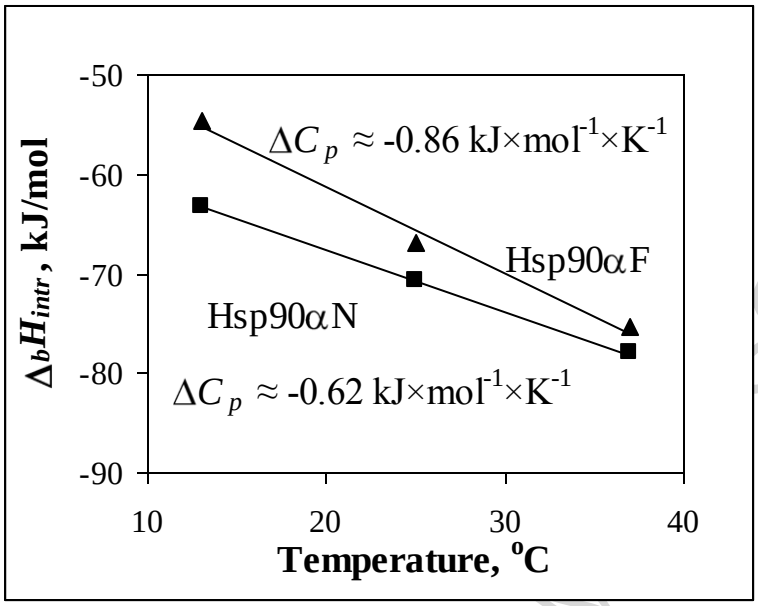

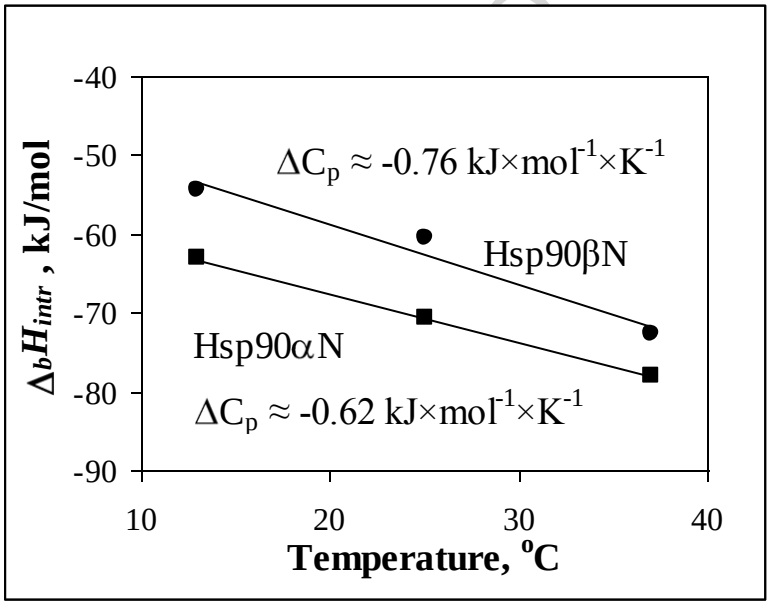

ACCEPTED MANUSCRIPT

Figure 4. Panels A and B

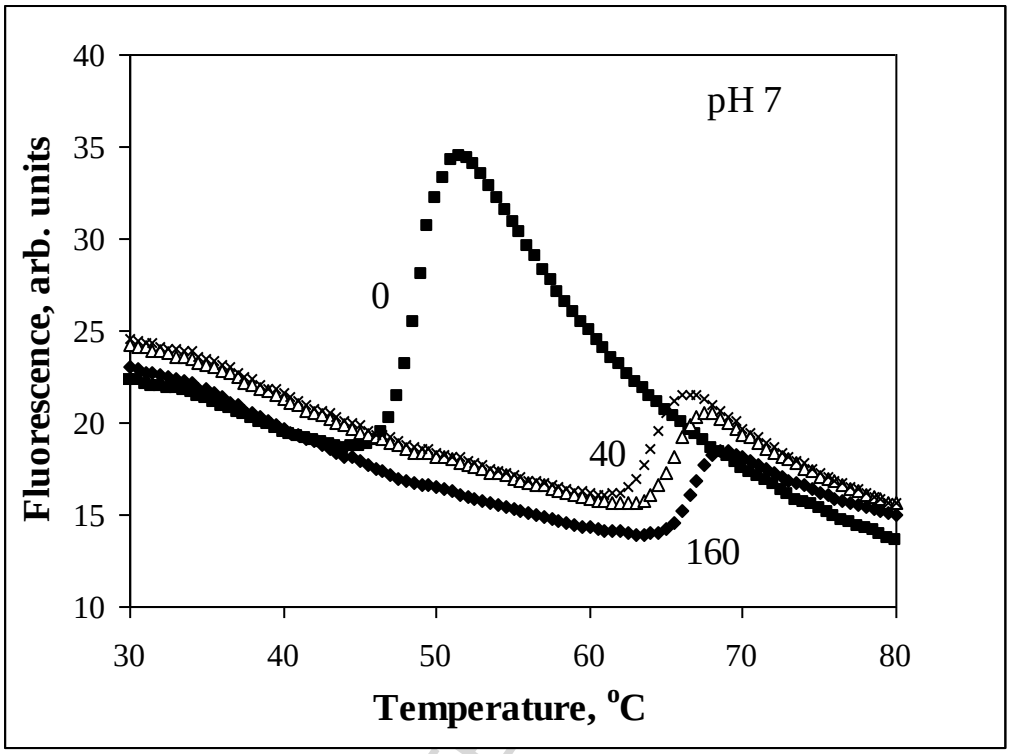

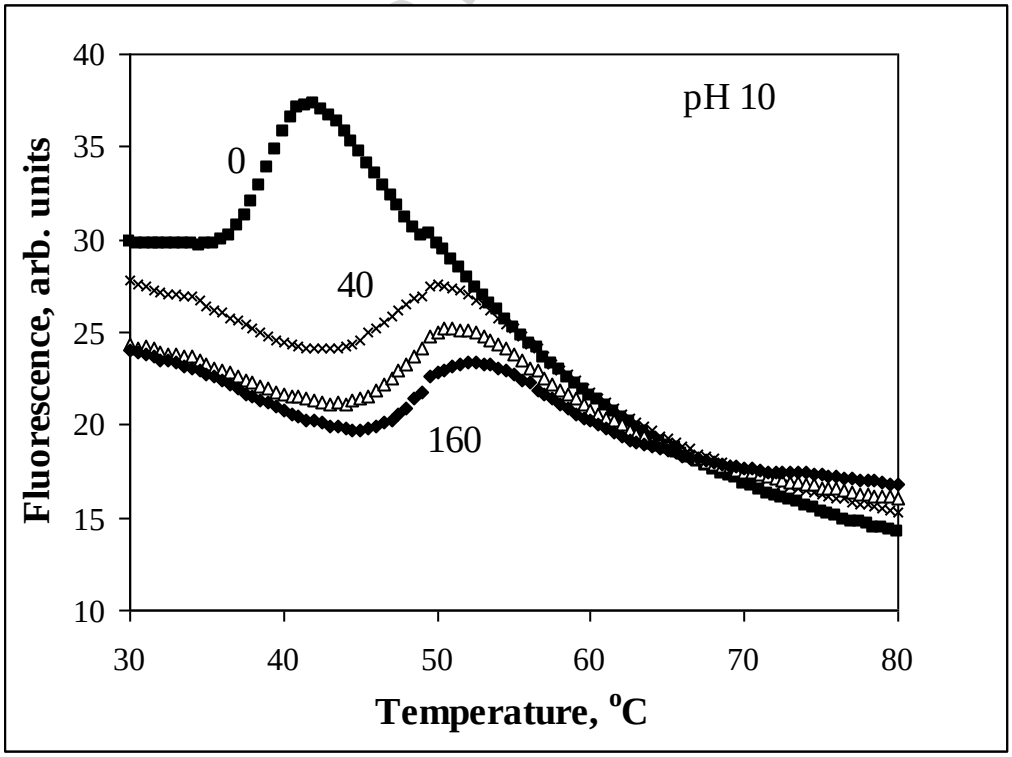

ACCEPTED MANUSCRIPT

Figure 4. Panel C

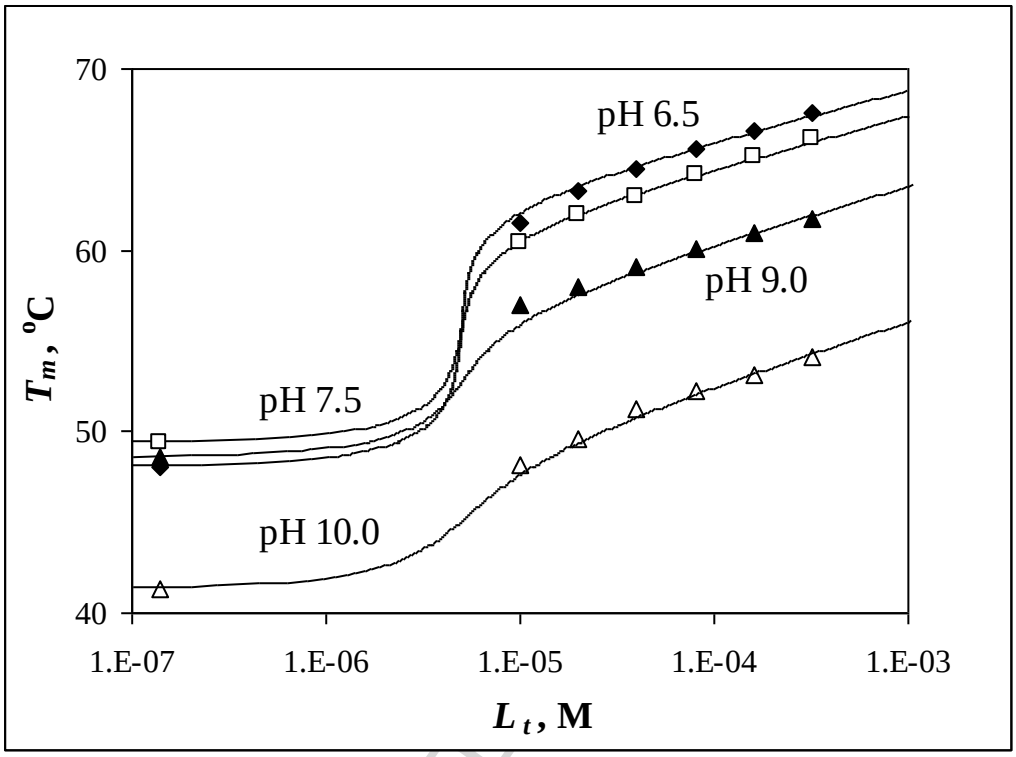

ACCEPTED

ACCEPTED MANUSCRIPT

Figure 5. Panels A and B

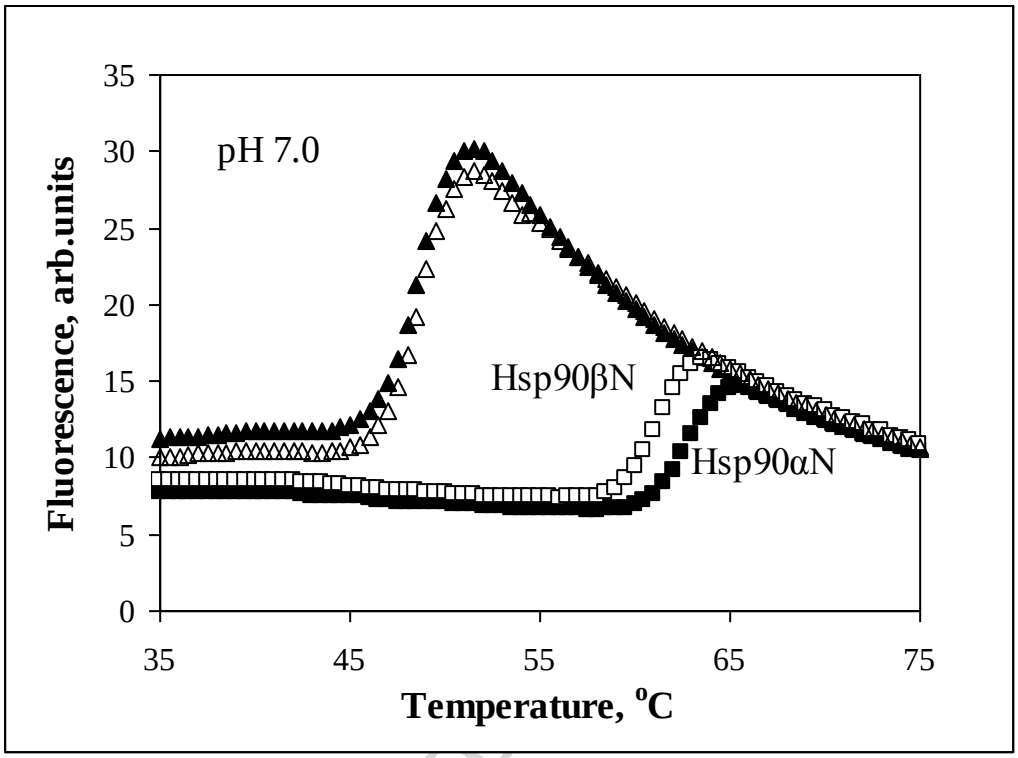

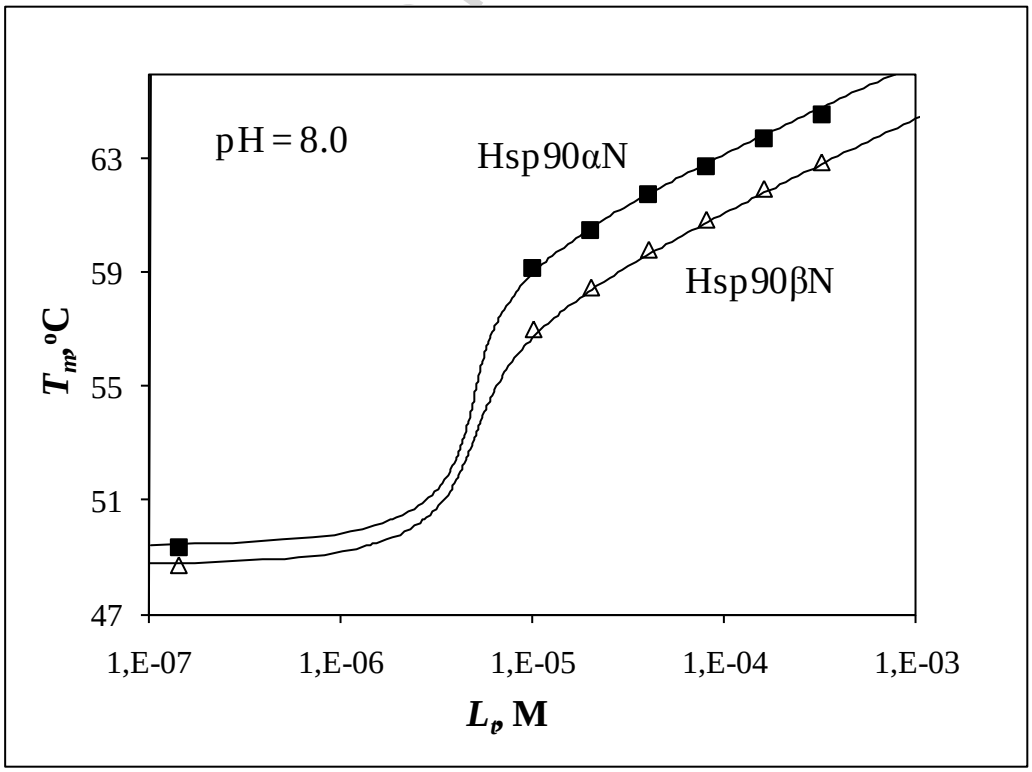

ACCEPTED MANUSCRIPT

Figure 6

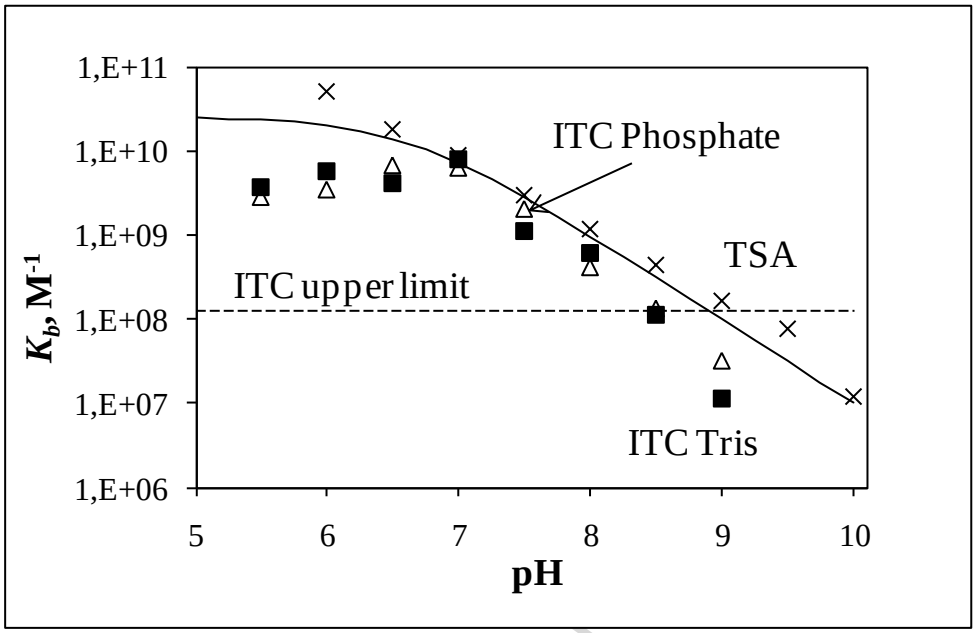

ACCEPTED M

ACCEPTED MANUSCRIPT

Figure 7. Panels A and B

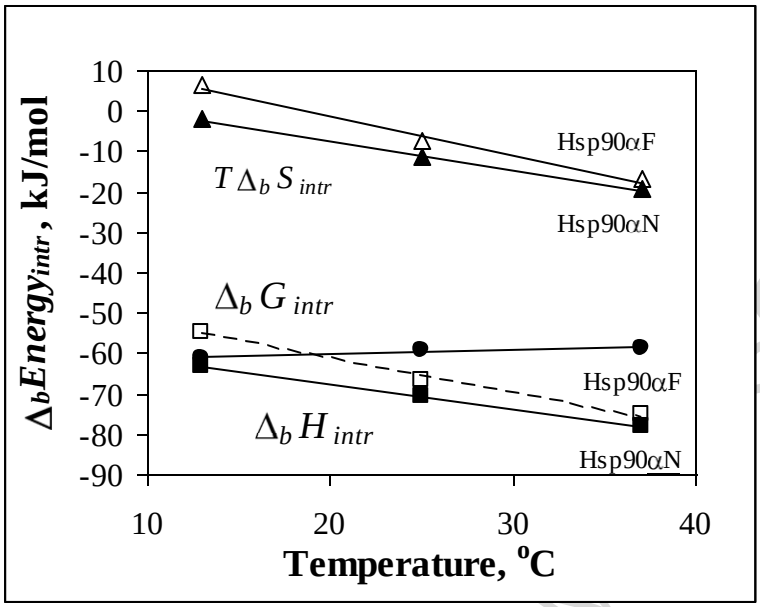

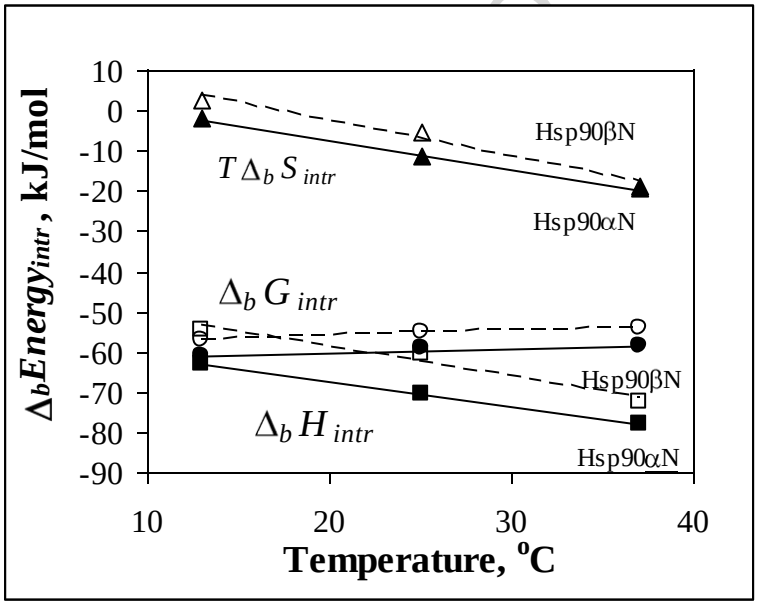

ACCEPTED MANUSCRIPT

Figure 8. Panel A:

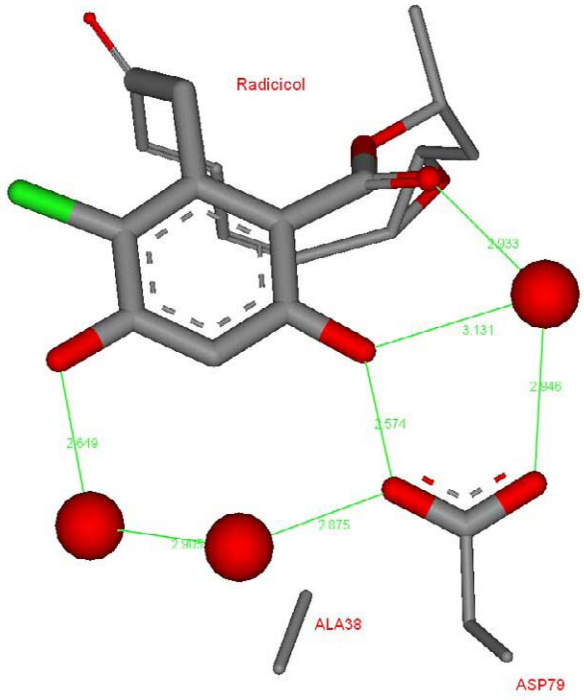

Panel B:

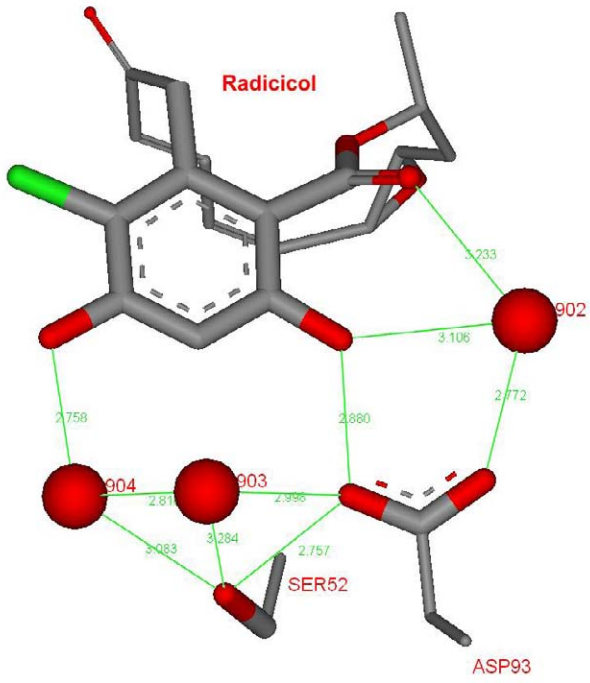

ACCEPTED MANUSCRIPT

Panel C

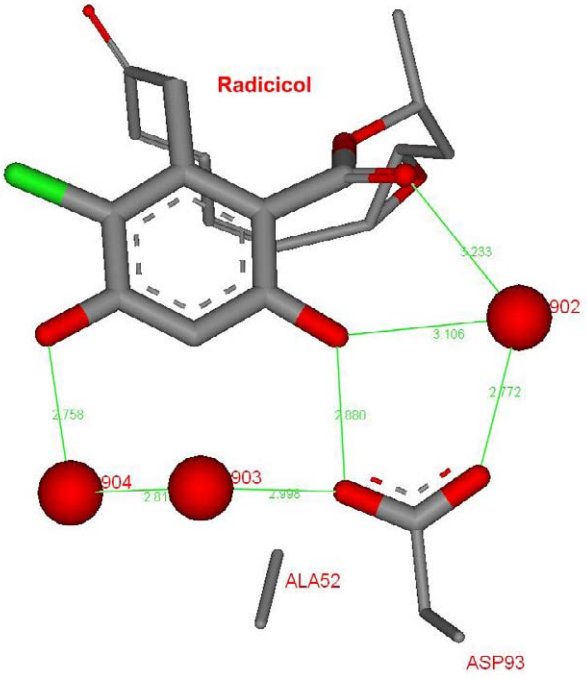

ACCEPTED MANUSCRIPT